

ЕЛЕКТРИЧНІ МАШИНИ ТА АПАРАТИ

УДК 621.313.8

DOI: <https://doi.org/10.15407/publishing2023.66.132>**THREE-DEGREE-OF-FREEDOM ELECTRIC MACHINE AND ITS OPERATION MODES****K.P. Akinin***, **V.G. Kireyev****, **I.S. Petukhov*****, **A.A. Filomenko******

Institute of Electrodynamics of the National Academy of Sciences of Ukraine,

Beresteyskiy ave., 56, Kyiv, 03057, Ukraine

e-mail: kvg2016@ukr.net

This paper deals with the operating modes of a 3-degree-of-freedom (3-DOF) electric machine. The design of such a machine allows the rotor axis to rotate along two angular coordinates in a limited range of angles. This is necessary for the machine to operate as part of a small-sized, high-speed precision target detection and tracking system. Based on the 3-DOF machine dynamics model, a block diagram of a servo system has been developed for controlling the rotor motion trajectory at two coordinates. Examples are given of the implementation of rotor motion trajectories with linearly increasing Examples are given of the implementation of rotor motion trajectories with linearly increasing, as well as described by an Archimedes spiral reference signals described by an Archimedes spiral reference signals. Dependencies of the modules of the relative accuracy of rotor movement along given trajectories on the system tunings were obtained. Ref. 12, fig. 9, table.

Keywords: control system, motion trajectories, three-degree-of-freedom electric machine.

Introduction. An electric machine with three degrees of freedom of rotor rotation is an electric motor whose rotor rotation axis can change its angular position in two mutually orthogonal planes relative to the stator windings. Such electric machines can differ not only by design, but also by implementation type: stepper [11], asynchronous [2, 3], inductor [1], with permanent magnets [4, 5]. In this paper brushless magnetoelectric motors with high-speed rotor with three degrees of freedom of rotation will be considered. Due to the rapid rotation of the rotor and the ability to tilt the axis of rotation in any direction, the rotor of such a machine has the properties of a gyroscope. It can maintain its spatial position in the absence of external influences on it, and in the presence of control torques, change the angular position of the rotation axis or, using the gyroscope term, precess.

A significant structural difference between a 3-DOF machine and traditional gyroscopic systems is the absence of an external gimbal suspension with angular position sensors and torque motors installed on its axes that control the position of the rotor axis of a special gyromotor. In the 3-DOF machine, all functions of controlling the rotor position and stabilizing its rotation are performed by a system of stator windings, the electromagnetic field of which interacts with the excitation field of a single rotor-magnet mounted on a miniature internal gimbal suspension. The advantages of this gyroscopic system structure in comparison with the classical scheme in speed, dimensions and weight with comparable values of the rotor angular momentum are obvious, since the angular momentum of the moving parts is significantly less. There is also no need to connect communications to the gyromotor, angle sensors and torque motors installed on the gimbal frames, which increases the reliability of the 3-DOF machine. However, these advantages are achieved by increasing the complexity of electrodynamic processes that occur in the 3-DOF machine and require special approaches to their study. The fundamentals of the 3-DOF theory machine were outlined in the monograph [5] and were continued in the monograph [4] and papers [6–8].

The purpose of the paper is to study the operating modes of the 3-DOF machine as part of small-sized, high-speed precision target detection and tracking systems.



Structure and operating principles of the 3-DOF machine. The 3-DOF machine is the main part of the electromechanical system for the spatial orientation of the sensitive element at two angular coordinates. Based on the tasks to be solved, three main operating modes can be defined:

- guidance of the sensitive element according to target designation signals;
- scanning space when searching for a target;
- holding the sight axis towards the target in tracking mode.

Before considering the modeling features and studying operating modes, we will briefly consider the 3-DOF machine design and describe the principles of its operation.

Structurally, the 3-DOF machine (Fig. 1) consists of a two-pole rotor with permanent magnets of the excitation system 1, a stator 2 with windings of rotor control in three angular coordinates, and a gimbal suspension 3. The magnetic flux of induction of the excitation system can be closed by outside and internal magnetic circuits 4, which rotate together with magnets. An important feature of the design is the absence of ferromagnetic elements on the stator. This eliminates the force interaction of the rotor magnets with the stator, which can cause unwanted rotor precession.

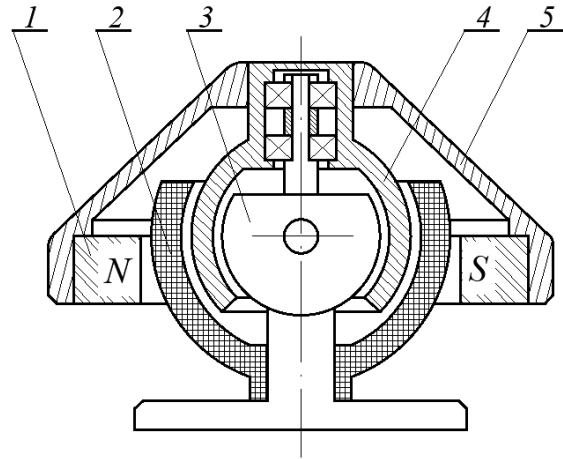


Fig. 1

Let's consider the principles of creating control torques along three angular coordinates in the 3-DOF machine. By analogy with classical electric machines for accelerating and stabilizing the rotor rotation speed, it is enough to install two mutually perpendicular rotation windings on the stator. In order to control the spatial position of the rotor rotation axis, an additional solenoidal control winding is mounted on the stator, the electrical axis of which is orthogonal to the rotation windings. In this case, an electromagnetic field appears in the working air gap of the machine, the intensity vector of which pulsates along the electrical axis of the control winding (CW). Fig. 2 shows the cross-section of the CW and rotor, as well as the fixed coordinate system of the stator $OXYZ$ and the movable $OX_1Y_1Z_1$ of the rotor, \mathbf{H}_{cw} is the instantaneous value of the vector of the field strength CW, \mathbf{H} is the vector of the angular momentum of the rotor, θ is the angle of deviation of the rotation axis rotor.

Due to the interaction of the excitation field of the rotor's permanent magnets, in which the magnetic induction vector \mathbf{B} coincides with the OZ_1 axis, and the field CW \mathbf{H}_{cw} , an electromagnetic torque \mathbf{M}_{cw} arises, directed along the OX axis. It has two components \mathbf{M}_{cw}^x – along the OX_1 axis and \mathbf{M}_{cw}^y – along the OY_1 axis. The first component of \mathbf{M}_{cw}^x is perpendicular to the vector of angular momentum \mathbf{H} , therefore, according to gyro theory [10], the rotor under the action of this torque will precess in the OY_1X_1 plane, trying to combine the vector \mathbf{H} with the torque vector \mathbf{M}_{cw}^x acting on the rotor. The \mathbf{M}_{cw}^y component and the vector of angular momentum \mathbf{H} are on the same axis, so no disturbing force is applied to the rotor, leading to precession. However, it tends to reduce the angular momentum of the rotor, which leads to its braking. When changing the direction of the \mathbf{H}_{cw} vector, that is when the direction of the current in the CW changes, the rotor will precess in the OZ_1Y_1 plane, and the \mathbf{M}_{cw}^y component will act in the same direction as the vector \mathbf{H} and increase the rotor rotation speed.

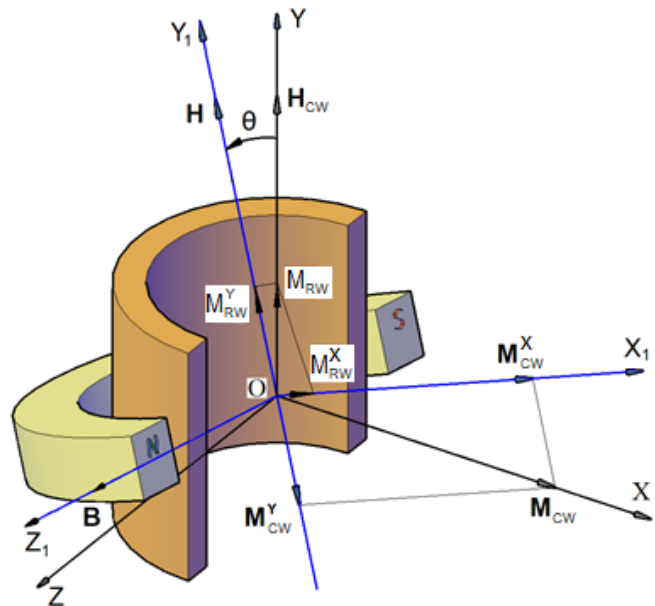


Fig. 2

Stabilizing the rotor's rotation speed is a prerequisite for the gyroscope to perform its functions, therefore it is necessary, using the rotation winding, to compensate for the disturbing effect of the CW, that is, to create an additional torque along the OY_1 axis equal in magnitude to M_{cw}^y and directed in the opposite direction. Since the electromagnetic torque M_{RW} created by the rotation windings (not shown in Fig. 2) is always directed along the OY axis, then to compensate for the torque M_{cw}^y it will require such a value, which at projection of the M_{RW} onto the OY_1 axis, would be equal and opposite to the vector M_{cw}^y . In this case, there also appears a projection of the torque vector M_{rw}^x on to the OX_1 axis, which acts in the same direction as the vector M_{cw}^x , increasing the torque of precession.

Thus, in the 3-DOF machine, there are cross-linkages between the processes of rotation and precession of the rotor along two axes. This is the main distinctive feature of the electrodynamic processes occurring in 3-DOF machine compared to classical electric machines. To develop the motor control system, use the physical model of the 3-DOF machine (Fig. 3) and the system of equations of its electrodynamic state, which were given in the monograph [4] and reflect the above features of the machine.

Fig. 3 presents the 3-DOF machine diagram in the form of three mutually orthogonal current

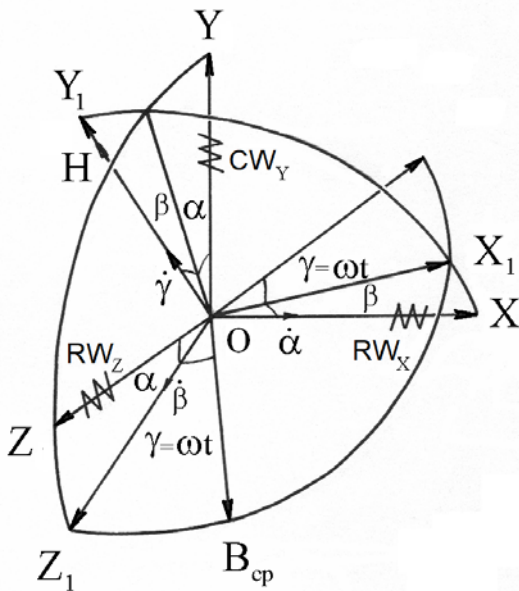


Fig. 3

circuits: windings of rotation RW_X , RW_Z and winding of control CW_Y , as well as a rotor magnetized along the vector B_{av} , which is orthogonal to the axis of its own rotation OY_1 . The coordinate system $OXYZ$ is fixed and connected to the stator windings, and $OX_1Y_1Z_1$ is the rotor coordinate system that is moving.

When compiling the model, some assumptions were made:

- there is no saturation of the magnetic circuit, which ensures a proportional dependence of all flux linkages and EMF on the corresponding currents in the windings;
- the current remains unchanged along the entire length of the winding conductor and therefore, to describe the energy of the electromagnetic field, lumped parameters of the circuit can be used - active and inductive resistance;
- we will consider a 3-DOF machine with a

two-pole rotor and carry out calculations based on the first harmonic;

- the use of highly coercive magnets in the excitation system determines the constancy of its magnetic characteristics when the external magnetic field of the stator windings varies, associated with changes in the currents flowing in them;

- since the 3-DOF machine (Fig. 1) does not contain ferromagnetic elements on the stator, and the magnetic axes of the control and rotation windings are mutually perpendicular, their mutual inductances are equal to zero;

- the center of rotation of the rotor is located at the intersection of the electrical axes of the rotation and control windings, which is ensured by the proper design of the gimbal suspension;

- the center of mass of the rotor coincides with the center of the suspension and its position remains unchanged when the rotor is tilted;

- the moments of inertia of the rotor J_X and J_Z relative to the equatorial axes OX_1 and OZ_1 , respectively, are equal to each other, since a rapidly rotating rotor is always a body of rotation.

Mathematical model and research results. Taking into account the accepted assumptions, the mathematical model of the 3-DOF machine has the form [4]

$$J_X \cos^2 \beta \frac{d\omega_\alpha}{dt} = -M_{Y\alpha} - M_{\omega\alpha} + M_{J\alpha} + M_{H\beta} + M_{Z\alpha}; \tag{1}$$

$$M_{Y\alpha} = i_Y k_{mY} (\sin \alpha \sin \beta \sin \omega t + \cos \alpha \cos \omega t); M_{\omega\alpha} = k_{\omega\alpha} \omega_\alpha; \tag{2, 3}$$

$$M_{J\alpha} = 2\omega_\alpha \omega_\beta J_X \sin \beta \cos \beta; M_{H\beta} = H \omega_\beta \cos \beta; \quad (4, 5)$$

$$M_{Z\alpha} = i_Z k_{mZ} (\sin \alpha \cos \omega t - \cos \alpha \sin \beta \sin \omega t); \quad (6)$$

$$J_X \frac{d\omega_\beta}{dt} = M_{Y\beta} - M_{\omega\beta} - M_{J\beta} - M_{H\alpha} - M_{X\beta} + M_{Z\beta}; \quad (7)$$

$$M_{Y\beta} = i_Y k_{mY} \cos \alpha \cos \beta \sin \omega t; M_{\omega\beta} = k_{\omega\beta} \omega_\beta; M_{J\beta} = \omega_\alpha^2 J_X \sin \beta \cos \beta; \quad (8-10)$$

$$M_{H\alpha} = H \omega_\alpha \cos \beta; M_{X\beta} = i_X k_{mX} \sin \beta \sin \omega t; M_{Z\beta} = i_Z k_{mZ} \sin \alpha \cos \beta \sin \omega t; \quad (11-13)$$

$$J_Y \frac{d\omega_\gamma}{dt} = -M_{X\gamma} - M_{Y\gamma} - M_{Z\gamma} + M_{L\gamma}; \quad (14)$$

$$M_{X\gamma} = i_X k_{mX} \cos \beta \cos \omega t; M_{Y\gamma} = i_Y k_{mY} (\cos \alpha \sin \beta \cos \omega t + \sin \alpha \sin \omega t); \quad (15, 16)$$

$$M_{Z\gamma} = i_Z k_{mZ} (\sin \alpha \sin \beta \cos \omega t - \cos \alpha \sin \omega t); M_{L\gamma} = k_{\omega\gamma} \omega_\gamma^2; \quad (17, 18)$$

$$\frac{d\alpha}{dt} = \omega_\alpha; \frac{d\beta}{dt} = \omega_\beta; \frac{d\gamma}{dt} = \omega_\gamma; \quad (19-20)$$

$$L_X \frac{di_X}{dt} = u_X - R_X i_X - e_{X\gamma} + e_{X\beta}; \quad (21)$$

$$e_{X\gamma} = \omega_\gamma k_{mX} \cos \beta \cos \omega t; e_{X\beta} = \omega_\beta k_{mX} \sin \beta \sin \omega t; \quad (22, 23)$$

$$L_Z \frac{di_Z}{dt} = u_Z - R_Z i_Z - e_{Z\gamma} - e_{Z\alpha} - e_{Z\beta}; \quad (24, 25)$$

$$e_{Z\gamma} = \omega_\gamma k_{mZ} (\sin \alpha \sin \beta \cos \omega t - \cos \alpha \sin \omega t); \quad (26)$$

$$e_{Z\alpha} = \omega_\alpha k_{mZ} (\cos \alpha \sin \beta \sin \omega t - \sin \alpha \cos \omega t); e_{Z\beta} = \omega_\beta k_{mZ} \sin \alpha \cos \beta \sin \omega t; \quad (27, 28)$$

$$L_Y \frac{di_Y}{dt} = u_Y - R_Y i_Y - e_{Y\gamma} + e_{Y\alpha} - e_{Y\beta}; \quad (29)$$

$$e_{Y\gamma} = \omega_\gamma k_{mY} (\cos \alpha \sin \beta \cos \omega t + \sin \alpha \sin \omega t); \quad (30)$$

$$e_{Y\alpha} = \omega_\alpha k_{mY} (\sin \alpha \sin \beta \sin \omega t + \cos \alpha \cos \omega t); e_{Y\beta} = \omega_\beta k_{mY} \cos \alpha \cos \beta \sin \omega t, \quad (31, 32)$$

where $\omega_\alpha, \omega_\beta, \omega_\gamma, \alpha, \beta, \gamma$ are angular speeds and angles of rotation of the rotor shaft; J_X, J_Y are axial moments of inertia of the rotor; $M_{Y\alpha}, M_{Y\beta}$ are electromagnetic torques created by the control winding; $M_{J\alpha}, M_{J\beta}$ are torques caused by Coriolis forces; $M_{H\alpha}, M_{H\beta}$ – cross gyroscopic torques; $M_{Z\alpha}, M_{X\beta}, M_{Z\beta}$ are electromagnetic torques caused by the influence of the rotation winding; $M_{X\gamma}, M_{Z\gamma}$ are electromagnetic torques of rotation windings; $M_{Y\gamma}$ is the electromagnetic torque caused by the influence of the control winding; $M_{L\gamma}$ is the torque of viscous friction; $k_{\omega\gamma}$ is the coefficient of viscosity of rotation of the motor rotor around the Y axis; $k_{\omega\alpha}, k_{\omega\beta}$ are viscosity coefficients when the rotor rotates through angles α and β , and $k_{\omega\alpha} = k_{\omega\beta}$; i_Y, u_Y are current and voltage of the control winding; i_X, i_Z, u_X, u_Z are currents and voltages of stator rotation windings; $L_Y, L_X, L_Z, R_Y, R_X, R_Z$ are inductance and active resistance of the control and rotation windings; $e_{X\gamma}, e_{X\beta}, e_{Z\gamma}, e_{Z\alpha}, e_{Z\beta}, e_{Y\gamma}, e_{Y\alpha}, e_{Y\beta}$ are EMF of rotation and control windings; k_{mY}, k_{mX}, k_{mZ} are the motor torque coefficients, and $k_{mX} = k_{mZ}$; $\omega = 2\pi f$ is the angular frequency; f is the currents frequency. You can see that all electromagnetic torques acting on the rotor are described by periodic functions, that is, they have variable components. Therefore, for further convenience of studying the dynamics of rotor motion, it is necessary to obtain the 3-DOF machine equations in average torque values.

Note also that, according to the conditions for rotor stabilization, the average value of the rotation rotor angular speed is constant $\omega_\gamma = \omega_{\gamma av} = 628 \text{ rad/s}$ at $f = 100 \text{ Hz}$. In this case, the sum

of the constant components of the torques $M_{X\gamma}$, $M_{Y\gamma}$, $M_{Z\gamma}$ and $M_{L\gamma}$ on the right side of equation (14) is always equal to zero. In this paper, the mode of stabilization of the angular speed of rotor rotation is not considered.

To obtain equations of dynamics in average values, it is necessary to determine formulas for currents i_X , i_Z and i_Y in the form

$$i_X = I_X \cos \omega t; \quad i_Z = I_Z \sin \omega t; \quad i_Y = I_Y \sin(\omega t + \varphi_Y), \quad (33-35)$$

where I_X , I_Z are the amplitudes of currents i_X and i_Z of rotation windings, and $I_X = I_Z$; I_Y , φ_Y are amplitude and phase shift of the control winding current i_Y .

Let's substitute expressions for currents into equations (2-6, 8-13, 15-18)

$$\begin{aligned} M_{Y\alpha} &= I_Y k_{mY} (\sin \alpha \sin \beta \sin \omega t + \cos \alpha \cos \omega t) \sin(\omega t + \varphi_Y) = \\ &= 0,5 I_Y k_{mY} (\sin \alpha \sin \beta (\cos \varphi_Y + \cos(2\omega t + \varphi_Y)) + \cos \alpha (\sin(2\omega t + \varphi_Y) + \sin \varphi_Y)); \end{aligned} \quad (36)$$

$$\begin{aligned} M_{Z\alpha} &= -I_Z k_{mZ} (\sin \alpha \cos \omega t - \cos \alpha \sin \beta \sin \omega t) \sin \omega t = \\ &= -I_Z k_{mZ} (0,5 \sin \alpha \sin 2\omega t - \cos \alpha \sin \beta \sin^2 \omega t); \end{aligned} \quad (37)$$

$$\begin{aligned} M_{Y\beta} &= I_Y k_{mY} \cos \alpha \cos \beta \sin(\omega t + \varphi_Y) \sin \omega t = \\ &= 0,5 I_Y k_{mY} \cos \alpha \cos \beta (\cos \varphi_Y + \cos(2\omega t + \varphi_Y)); \end{aligned} \quad (38)$$

$$M_{X\beta} = I_X k_{mX} \sin \beta \sin \omega t \cos \omega t = 0,5 I_X k_{mX} \sin \beta \sin 2\omega t; \quad (39)$$

$$M_{Z\beta} = -I_Z k_{mZ} \sin \alpha \cos \beta \sin^2 \omega t; \quad (40)$$

$$M_{X\gamma} = I_X k_{mX} \cos \beta \cos^2 \omega t; \quad (41)$$

$$\begin{aligned} M_{Y\gamma} &= I_Y k_{mY} (\cos \alpha \sin \beta \cos \omega t + \sin \alpha \sin \omega t) \sin(\omega t + \varphi_Y) = \\ &= 0,5 I_Y k_{mY} (\cos \alpha \sin \beta (\sin(2\omega t + \varphi_Y) + \sin \varphi_Y) + \sin \alpha (\cos \varphi_Y + \cos(2\omega t + \varphi_Y))); \end{aligned} \quad (42)$$

$$\begin{aligned} M_{Z\gamma} &= -I_Z k_{mZ} (\sin \alpha \sin \beta \cos \omega t - \cos \alpha \sin \omega t) \sin \omega t = \\ &= -I_Z k_{mZ} (0,5 \sin \alpha \sin \beta \sin 2\omega t - \cos \alpha \sin^2 \omega t); \end{aligned} \quad (43)$$

Eliminating from equations (36-43) variable components whose average values are equal to zero, one can finally write down formulas for electromagnetic torques in average values

$$M_{Y\alpha} = 0,5 I_Y k_{mY} (\sin \alpha \sin \beta \cos \varphi_Y + \cos \alpha \sin \varphi_Y); \quad (44)$$

$$M_{Z\alpha} = 0,5 I_Z k_{mZ} \cos \alpha \sin \beta; \quad M_{Y\beta} = 0,5 I_Y k_{mY} \cos \alpha \cos \beta \cos \varphi_Y; \quad (45, 46)$$

$$M_{X\beta} = 0; \quad M_{Z\beta} = -0,5 I_Z k_{mZ} \sin \alpha \cos \beta; \quad M_{X\gamma} = 0,5 I_X k_{mX} \cos \beta; \quad (47-49)$$

$$M_{Y\gamma} = 0,5 I_Y k_{mY} (\cos \alpha \sin \beta \sin \varphi_Y + \sin \alpha \cos \varphi_Y); \quad M_{Z\gamma} = -0,5 I_Z k_{mZ} \cos \alpha; \quad (50, 51)$$

Considering that the angular rotor movement is carried out in a relatively small angular range, the following substitutions can be made: $\sin \alpha = \alpha$, $\sin \beta = \beta$, $\cos \alpha = 1$ and $\cos \beta = 1$. Then the equations for torques (2, 4-6, 8, 10, 12, 13, 15-17, 44-51) can be simplified

$$M_{J\alpha} = 2\omega_\alpha \omega_\beta J_X \beta; \quad M_{H\beta} = H \omega_\beta; \quad M_{J\beta} = \omega_\alpha^2 J_X \beta; \quad M_{H\alpha} = H \omega_\alpha; \quad (52-55)$$

$$M_{Y\alpha} = 0,5 I_Y k_{mY} (\alpha \beta \cos \varphi_Y + \sin \varphi_Y); \quad M_{Z\alpha} = 0,5 I_Z k_{mZ} \beta; \quad M_{Y\beta} = 0,5 I_Y k_{mY} \cos \varphi_Y; \quad (56-58)$$

$$M_{X\beta} = 0; \quad M_{Z\beta} = -0,5 I_Z k_{mZ} \alpha; \quad M_{X\gamma} = 0,5 I_X k_{mX} \cos \beta; \quad (59-61)$$

$$M_{Y\gamma} = 0,5 I_Y k_{mY} (\beta \sin \varphi_Y + \alpha \cos \varphi_Y); \quad M_{Z\gamma} = -0,5 I_Z k_{mZ}. \quad (62, 63)$$

Preliminarily neglecting the insignificant torques $M_{J\alpha}$ and $M_{J\beta}$, as well as the first term in equation (56), we write equations (1, 7, 14) of dynamics in the form

$$J_X \frac{d\omega_\alpha}{dt} = -0,5 I_Y k_{mY} \sin \varphi_Y - k_{\omega\alpha} \omega_\alpha + H \omega_\beta + 0,5 I_Z k_{mZ} \beta; \quad (64)$$

$$J_X \frac{d\omega_\beta}{dt} = 0,5I_Y k_{mY} \cos \varphi_Y - k_{\omega\beta} \omega_\beta - H\omega_\alpha - 0,5I_Z k_{mZ} \alpha; \tag{65}$$

$$0,5I_Y k_{mY} (\beta \sin \varphi_Y + \alpha \cos \varphi_Y) + 0,5I_X k_{mX} + 0,5I_Z k_{mZ} = M_{LY}. \tag{66}$$

Since $I_X = I_Z$ and $k_{mX} = k_{mZ}$, then based on (66) it is possible to determine the current amplitude I_X depending on the changing control current i_Y

$$I_X = \frac{M_{LY} - 0,5I_Y k_{mY} (\beta \sin \varphi_Y + \alpha \cos \varphi_Y)}{k_{mX}}. \tag{67}$$

In equations (64, 65) you can notice that the control action in the system is the current components i_Y

$$I_{Y\alpha} = I_Y \sin \varphi_Y; I_{Y\beta} = I_Y \cos \varphi_Y. \tag{68, 69}$$

Taking into account (68, 69), we write equations (64-66) in the form

$$J_X \frac{d\omega_\alpha}{dt} = -0,5k_{mY} I_{Y\alpha} - k_{\omega\alpha} \omega_\alpha + H\omega_\beta + 0,5I_Z k_{mZ} \beta; \tag{70}$$

$$J_X \frac{d\omega_\beta}{dt} = 0,5k_{mY} I_{Y\beta} - k_{\omega\beta} \omega_\beta - H\omega_\alpha - 0,5I_Z k_{mZ} \alpha; \tag{71}$$

$$I_X = \frac{M_{LY} - 0,5k_{mY} (I_{Y\alpha} \beta + I_{Y\beta} \alpha)}{k_{mX}}. \tag{72}$$

According to the system of equations (70-72), Fig. 4 presents a block diagram, which also shows the transfer functions of the controllers $W_C(p)$ and rotor angular position sensors $W_S(p)$. There is also a designation $k_1 = 0,5I_X k_{mZ}$ in the diagram.

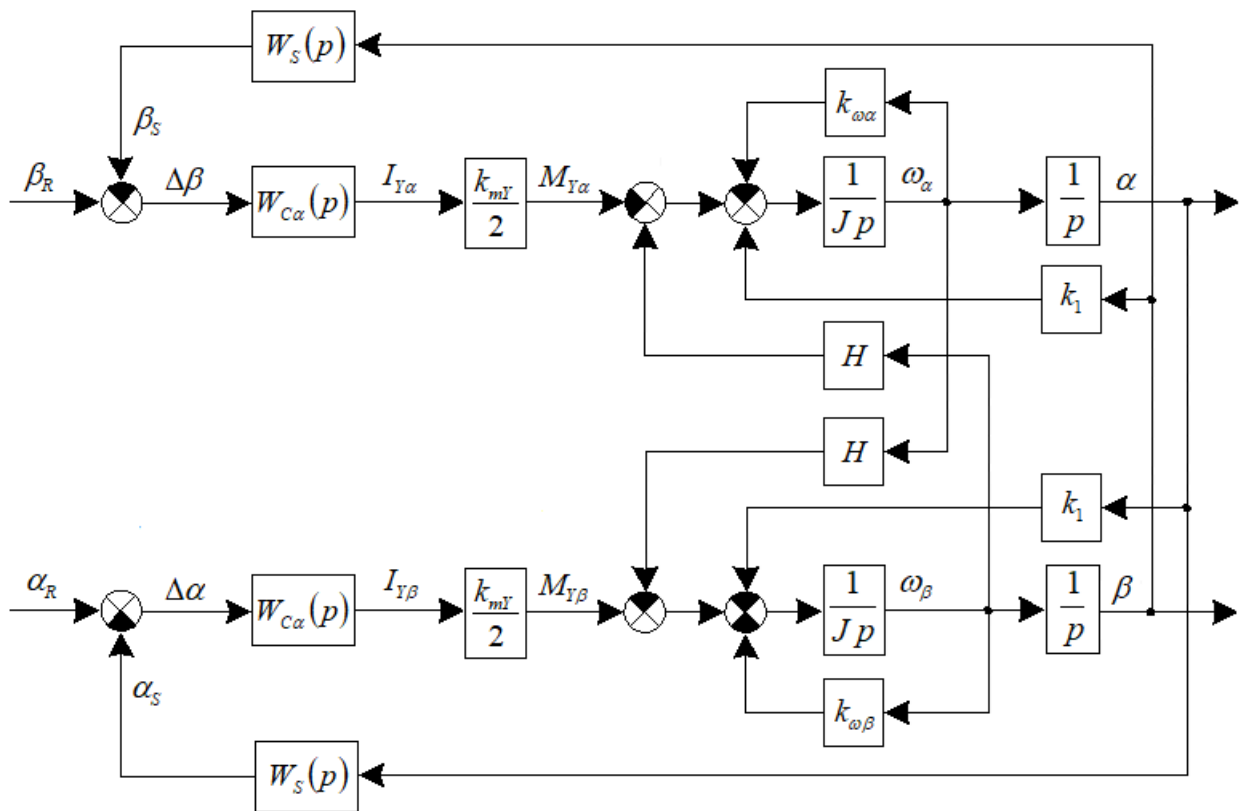


Fig. 4

When developing a system for controlling rotor rotation angles α and β , Hall sensors are used, for which the rated response time is 0.000003 s, therefore its transfer function with the output signal was presented in the form of a first-order aperiodic link

$$W_s(p) = \frac{1}{T_s p + 1} \quad (73)$$

with time constant $T_s = 0,000001 \text{ s}$.

In addition, it is assumed that current control of the rotor rotation angles α and β is implemented, that is, the influence of the internal electromotive forces of circuits and the electromagnetic time constants of the 3-DOF machine windings are compensated.

Based on the structure (Fig. 4), we obtain the transfer function of the open-loop system

$$W_{OLS}(p) = \left(W_C(p) \frac{0,5k_{mY}}{p(T_J p + 1)k_{\omega\alpha}} \right)^2 \left(W_s(p) + \frac{pH + k_1}{0,5k_{mY}W_C(p)} \right)^2, \quad (74)$$

where $T_J = \frac{J}{k_{\omega\alpha}}$.

The structure (Fig. 4) is characterized by the following parameters: $H = 0,02405 \text{ kg m}^2 / \text{s}$, $J = J_X = J_Z = 3,06 \cdot 10^{-5} \text{ kg m}^2$, $J_Y = 3,83 \cdot 10^{-5} \text{ kg m}^2$, $k_{mX} = k_{mZ} = 0,02388 \text{ Nm} / \text{A}$, $k_{mY} = 0,06154 \text{ Nm} / \text{A}$, $k_{\omega\alpha} = k_{\omega\beta} = 9,62 \cdot 10^{-3} \text{ Nm s} / \text{rad}$, $M_{LY} = 5 \cdot 10^{-5} \text{ Nm}$, $T_s = 10^{-6} \text{ s}$, $T_J = 3,181 \cdot 10^{-3} \text{ s}$.

When developing approaches to calculating the rotor rotation control system, we neglect the parameters T_s and k_1 due to their insignificant influence on dynamic processes, however, in the future, when modeling dynamic processes, all these factors will be taken into account.

To develop the control system, we select a proportional-integral (PI) controller

$$W_C(p) = k_C \frac{T_C p + 1}{p}, \quad (75)$$

where k_C , T_C are the gain and time constant of the PI controller.

In this case, the transfer function of the open-loop system has the form

$$W_{OLS}(p) = \left(\frac{k_2 \left(\frac{H}{k_2} p^2 + T_C p + 1 \right)}{p^2 (T_J p + 1) k_{\omega\alpha}} \right)^2 = \left(\frac{k_2 (T_1 p + 1) (T_2 p + 1)}{p^2 (T_J p + 1) k_{\omega\alpha}} \right)^2, \quad (76)$$

where

$$k_2 = 0,5k_{mY}k_C. \quad (77)$$

Time constants T_1 and T_2 are determined by the formulas

$$T_1 = \frac{2 \frac{H}{k_2}}{T_C - \sqrt{T_C^2 - 4 \frac{H}{k_2}}} \quad \text{and} \quad T_2 = \frac{2 \frac{H}{k_2}}{T_C + \sqrt{T_C^2 - 4 \frac{H}{k_2}}}. \quad (78, 79)$$

For the transfer function of an open-loop system (76), one can obtain the magnitude and phase frequency transfer functions

$$A(\omega) = \frac{k_{OLS}^2 (T_1^2 \omega^2 + 1) (T_2^2 \omega^2 + 1)}{\omega^4 (T_J^2 \omega^2 + 1)}; \quad A_L(\omega) = 20 \log A(\omega); \quad (81, 82)$$

$$\varphi(\omega) = -2\pi - 2\arctg \omega T_J + 2\arctg \omega T_1 + 2\arctg \omega T_2, \quad (83)$$

where

$$k_{OLS} = \frac{0,5k_{mY}k_C}{k_{\omega\alpha}} \quad (84)$$

is the gain of the open-loop system.

The condition for tuning a stable control system is to make a sufficient phase stability margin at the cut-off frequency ω_C [12]. The phase stability margin γ_C is determined in accordance with the frequency response

$$\gamma(\omega) = \pi + \varphi(\omega) = -\pi - 2\arctg\omega T_J + 2\arctg\omega T_1 + 2\arctg\omega T_2. \quad (85)$$

Ensuring a sufficient phase stability margin $\gamma_C = \gamma(\omega_C)$ is possible by choosing a certain ratio of the time constants T_2 and T_J under the condition $T_J < T_2$. In the future, it will be possible to notice that the accuracy of the choice of value T_1 is not so critical when tuning the system, since the sum of the terms $-\pi + 2\arctg\omega T_1$ is to be practically equal to zero in the high-frequency part of the frequency response. Fig. 5 shows phase frequency response

$$\varphi_1(\omega) = -2\arctg\omega T_J + 2\arctg\omega T_2, \quad (86)$$

which demonstrate the effect of ensuring a phase margin, while the following relationships between time constants were chosen: $1,6T_J$, $2T_J$, $2,4T_J$, $2,8T_J$ and $3,2T_J$, which are indicated in the figure, respectively, by numbers from 1 to 5.

Fig. 6 shows an example of magnitude $A_L(\omega)$ and phase $\gamma(\omega)$ Bode plots for a stable system at $T_2 = 2T_J$ and $T_C = 0,1$ s.

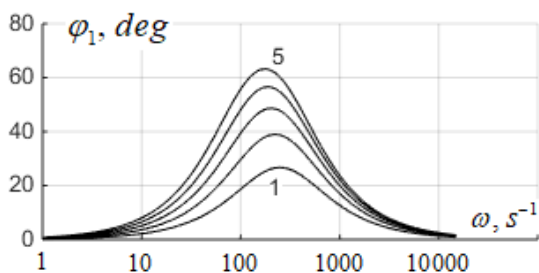


Fig. 5

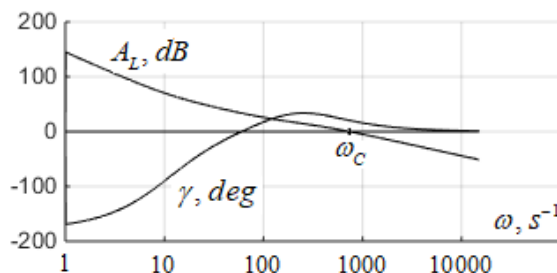


Fig. 6

Analysis of the transfer function $W_{OLS}(p)$ of the open-loop system and dependencies (78, 79) taking into account the curves (Fig. 5) shows that tuning the system can be done by choosing the desired value of the time constant T_2 . Then, taking into account the selected value of the time constant T_C of the PI controller and formula (79), it is possible to determine the gain k_2 (77)

$$k_2 = \frac{H}{T_2(T_C - T_2)}. \quad (87)$$

The value T_1 can then be determined using formula (78).

The table presents the results of calculating the system parameters T_1 and k_{OLS} , cut-off frequency ω_C and phase margin γ_C depending on the accepted desired values of the time constants T_2 and T_C . For the obtained system tunings, the following performance indexes of the operating mode were calculated: the effective value I of the control winding current, as well as the absolute maximum error values

$$\varepsilon_\beta = \beta_R - \beta \quad \text{and} \quad \varepsilon_\alpha = \alpha_R - \alpha \quad (88, 89)$$

with reference signals in the form

$$\beta_R = \alpha_A \sin \omega_R t; \quad \alpha_R = 0. \quad (90, 91)$$

The reference signal (90) and all subsequent options for calculating the dynamics of the system were carried out while limiting the maximum values of angular speeds ω_α and ω_β by the value $\omega_{\max} = 1 \text{ rad/s}$. That is, the reference signal parameter ω_R is defined as

$$\omega_R = \frac{\omega_{\max}}{\alpha_A}. \quad (92)$$

The effective value I of the control winding current is determined according to the formula for the current i_Y (35), where its amplitude and phase shift are

$$I_Y = \sqrt{I_{Y\alpha}^2 + I_{Y\beta}^2} \text{ and} \quad (93)$$

$$\varphi_Y = \arctg \frac{I_{Y\alpha}}{I_{Y\beta}} \text{ at } I_{Y\beta} > 0 \text{ or } \varphi_Y = \frac{\pi}{2} + \arctg \frac{I_{Y\alpha}}{I_{Y\beta}} \text{ at } I_{Y\beta} < 0. \quad (94)$$

T_C, s	T_2, s	T_1, s	k_{OLS}	ω_C, s^{-1}	γ_C, deg	I, A	ε_β, rad	ε_α, rad
0,05	$1,6T_J$	0,04491	10938	749,65	12,73	0,2225	0,004505	0,001973
	$2T_J$	0,04364	9005,3	739,9	18,505	0,2245	0,005518	0,002425
	$2,4T_J$	0,04236	7729,8	734,3	22,44	0,2261	0,006475	0,002848
	$2,8T_J$	0,04109	6830,6	730,9	25,27	0,2273	0,007370	0,003227
	$3,2T_J$	0,03982	6167,8	728,6	27,37	0,2281	0,008198	0,003569
0,1	$1,6T_J$	0,09491	5175,6	749,35	14,52	0,2135	0,004800	0,001997
	$2T_J$	0,09364	4196,7	739,55	20,41	0,2130	0,005919	0,002437
	$2,4T_J$	0,09237	3545,4	734,0	24,44	0,2121	0,006993	0,002837
	$2,8T_J$	0,09109	3081,4	730,5	27,37	0,2107	0,008014	0,003191
	$3,2T_J$	0,08982	2734,4	728,2	29,58	0,2089	0,008976	0,003497
0,2	$1,6T_J$	0,1949	2520,2	749,3	15,35	0,2082	0,004885	0,001973
	$2T_J$	0,1936	2029,4	739,5	21,26	0,2064	0,006031	0,002393
	$2,4T_J$	0,1924	1702,4	733,9	25,33	0,2041	0,007132	0,002767
	$2,8T_J$	0,1911	1468,9	730,45	28,27	0,2013	0,008178	0,003089
	$3,2T_J$	0,1898	1293,9	728,15	30,51	0,1980	0,009161	0,003360

Fig. 7 shows an example of calculating the transient responses of rotation angles α and β , current components of the control winding $I_{Y\alpha}$ and $I_{Y\beta}$, angular speeds ω_α and ω_β , errors of the processing reference signals ε_β and ε_α , as well as the current i_Y in the control winding. The calculation was performed using the reference signals (90, 91) and parameters $T_2 = 2T_J$ and $T_C = 0,1 s$, as well as $\alpha_A = \pi/180$ and $\omega_R = 57,297 s^{-1}$.

Fig. 8 shows an example of calculating the same transient responses with a linearly increasing and limited reference signal

$$\frac{d\beta_R}{dt} = \omega_{\max} \text{ and if } \beta_R > \alpha_A, \text{ then } \beta_R = \alpha_A; \quad (95)$$

$$\alpha_R = 0. \quad (96)$$

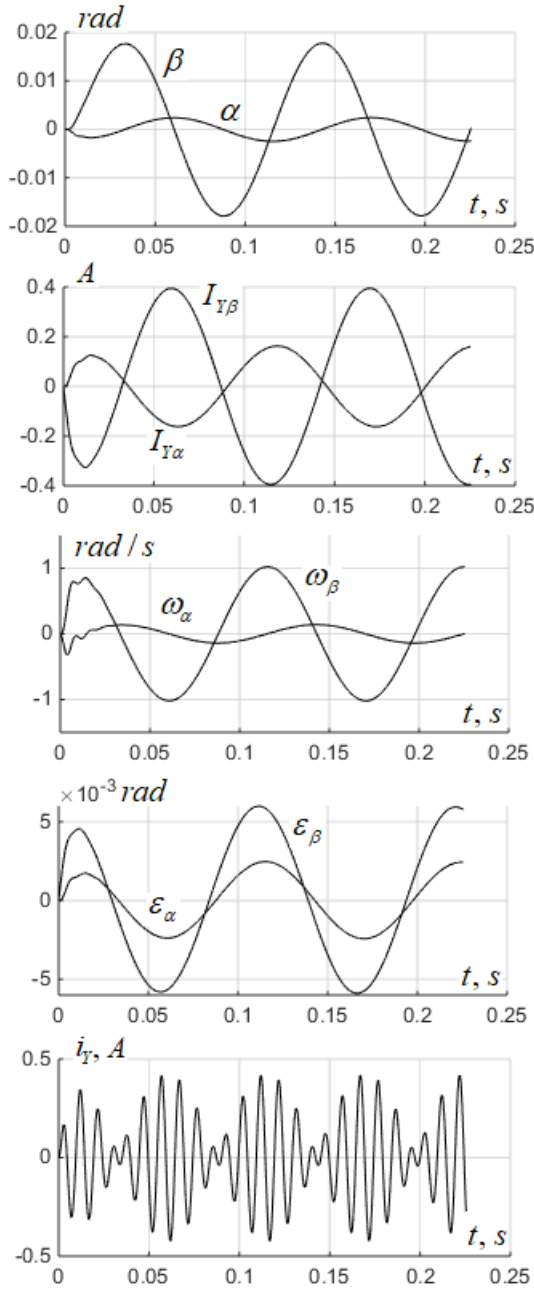


Fig. 7

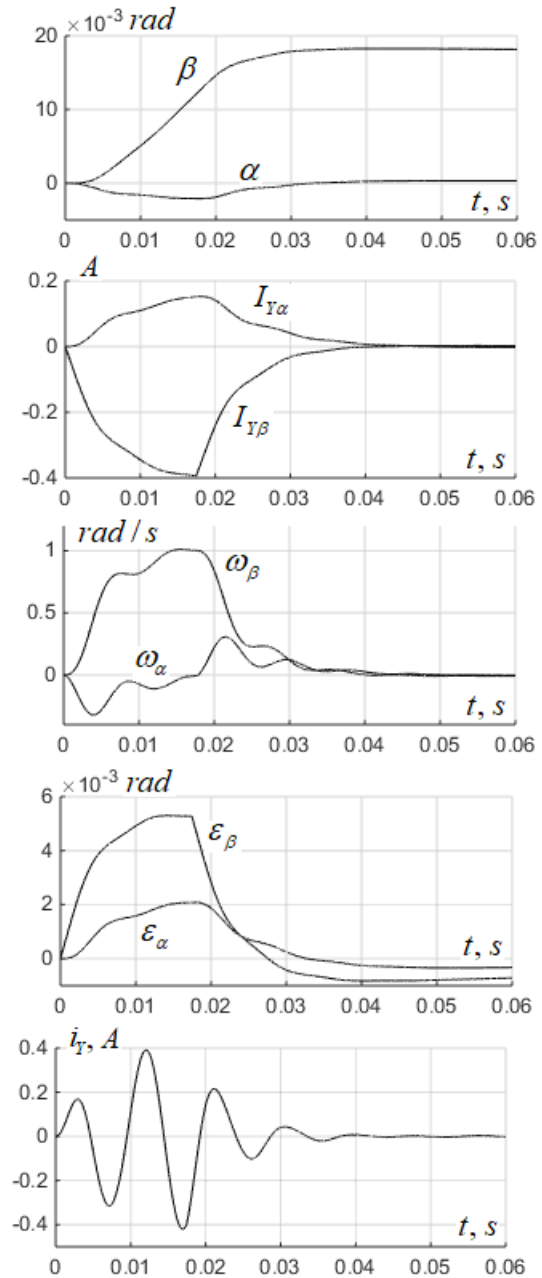


Fig. 8

Another dynamic mode of operation of the 3-DOF machine is a motion trajectory processing, which is described by an Archimedes spiral, subject to limited angular speeds ω_α and ω_β at a given maximum level $\omega_{\max} = 1 \text{ s}^{-1}$

$$\frac{d\theta}{dt} = \omega_R; \tag{97}$$

$$\text{if } \theta > 2\pi n, \text{ then } N = 1 \text{ or if } \theta > 4\pi n, \text{ then } N = 0 \text{ and } \theta = 0; \tag{98}$$

$$\alpha_A = |B\theta - N\theta_{\max}|; \tag{99}$$

$$\omega_R = \frac{\omega_{\max}}{\alpha_A}, \text{ if } \omega_R > \omega_{R\max}, \text{ then } \omega_R = \omega_{R\max}; \tag{100}$$

$$\alpha_R = \alpha_A \sin \theta; \beta_R = \alpha_A \cos \theta, \tag{101, 102}$$

where θ is the angle of rotation along the spiral of the inclined axis OY of the motor rotor; n is number of turns of the spiral; $\theta_{\max} = 2\pi n$ is the maximum angle of rotation when making n spiral

turns; $B = \frac{\alpha_{A\max}}{2\pi n}$ is the indicator of the increase in the angle of deviation of the rotor axis during spiral rotation; N is the parameter for the formation of increasing ($N = 0$) and decreasing ($N = 1$) sections of the spiral; $\omega_{R\max}$ is the maximum frequency value in the vicinity of a point with zero coordinates, we assume $\omega_{R\max} = 628 \text{ s}^{-1}$.

Fig. 9 presents the results of calculating the transient responses of the main variables of the dynamic process of movement along a trajectory in the form of an Archimedes spiral at $n = 10$ and $\alpha_{A\max} = \pi/18$.

Over the entire interval of processing such a trajectory, the effective value of the control winding current is $I = 0,3019 \text{ A}$.

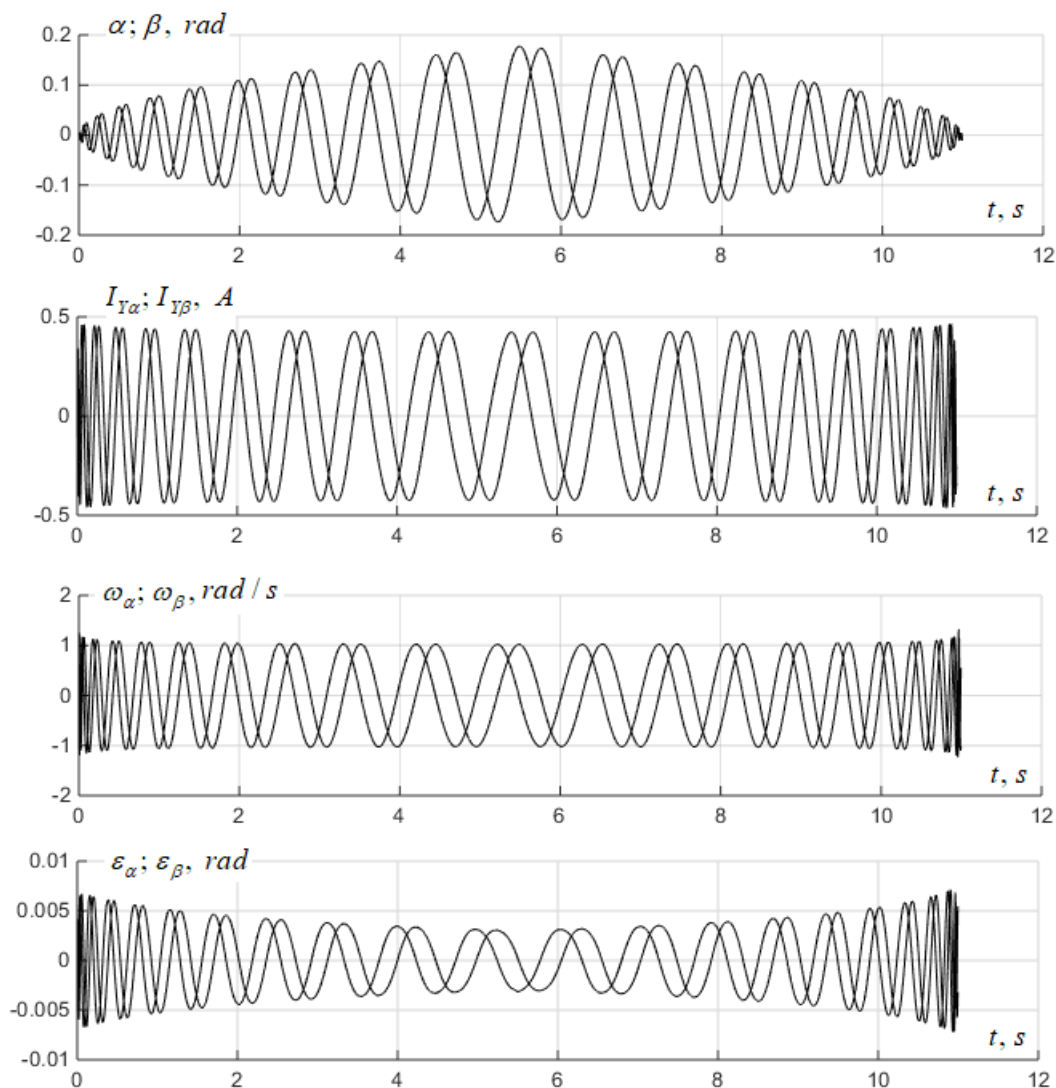


Fig. 9

Conclusions. The study of dynamic processes of a 3-DOF machine has shown that, for given parameters, the value of the time constant T_C of the PI controller in the selected range has practically no effect on the performance indexes of the operating mode. For different selected values of the time constant T_C , the difference between the effective value I of the control winding current and the absolute maximum error values ε_β and ε_α (Table) is no more than 11 percent. At the same time, it is the selected value of the time constant T_2 that determines the quality of the

operating mode of the 3-DOF machine, namely, that it has a significant impact on the phase margin γ_C and the error values ε_β and ε_α . In this case, the value of the cut-off frequency is determined with high accuracy by the ratio of the time constants T_2 and T_J .

Фінансується за держбюджетною темою «Розробити наукові засади та принципи побудови керованих *n*-ступеневих магнітоелектричних систем з екстремальними характеристиками» (шифр «Екстремум»), що виконується за Постановою Бюро ВФТПЕ 29.05.2018 р., протокол № 9. Державний реєстраційний номер роботи 0119U001279. КПКВК 6541030.

1. Wenqiang Tao, Guoli Li, Lufeng Ju, Rui Zhou, Cungang Hu Design and Analysis of a Novel Spherical Motor Based on the Principle of Reluctance. *2018 IEEE International Power Electronics and Application Conference and Exposition*. 2018. Pp. 7–13. DOI: <https://doi.org/10.1109/PEAC.2018.8590483>
2. Lee H.J., Park H.J., Ryu G.H., Oh S.Y., Lee J. Performance Improvement of Operating Three-Degree-of-Freedom Spherical Permanent-Magnet Motor. *IEEE Transactions on magnetics*. 2012. Vol. 48. No. 11. Pp. 4654–4657. DOI: <https://doi.org/10.1109/TMAG.2012.2200470>
3. Yan Wen, Guoli Li, Qunjing Wang, Xiwen Guo, Wenping Cao Modeling and Analysis of Permanent Magnet Spherical Motors by a Multitask Gaussian Process Method and Finite Element Method for Output Torque. *IEEE Transactions on Industrial Electronics*. 2021. Vol. 68. Issue 9. Pp. 8540–8549. DOI: <https://doi.org/10.1109/TIE.2020.3018078>
4. Antonov A.E. Electrical machines of magnetoelectric type. Kiev: NAS of Ukraine, Institute of Electrodynamics, 2011. 216 p. (Rus)
5. Milyakh A.N., Barabanov V.A., Dvoinykh V.V. Three-degree-of-freedom electric machines. Kyiv: Naukova Dumka, 1979. 308 p. (Rus)
6. Milyakh A.N., Barabanov V.A., Lavrinenko V.A., Kireev V.G. Equations of three-degree-of-freedom electric machines with permanent magnets. *Tekhnichna elektrodynamika*. 1981. No. 2. P. 65–70. (Rus)
7. Akinin K.P., Kireev V.G., Petukhov I.S., Filomenko A.A. Mathematical modeling of an electric machine with a three-degree-of-freedom gyro-stabilized rotor. *Tekhnichna elektrodynamika*. 2022. No 5. P. 38–44. (Ukr)
8. Petukhov I.S. Electromagnetic torques of control of the precession rotor of a three-degree-of-freedom electric machine. *Tekhnichna elektrodynamika*. 2023. No 4. P. 52–61. (Ukr)
9. Carrier G.F., Miles J.W. About the ring damper of a free precessing gyroscope. *Applied mechanics*. Series E. 1963. No 2. (Rus)
10. Siff E.J., Emmerich K.L. Introduction to gyroscopy. M.: Mechanical Engineering, 1965. 124 p. (Rus)
11. Wen Y., Li G., Wang Q., Guo X., Cao W. Modeling and Analysis of Permanent Magnet Spherical Motors by a Multitask Gaussian Process Method and Finite Element Method for Output Torque. *IEEE Transactions on Industrial Electronics*. 2021. Vol. 68. Issue 9. Pp. 8540–8549. DOI: <https://doi.org/10.1109/TIE.2020.3018078>
12. Viteček A., Vitečková M., Landryová L. Basic principles of automatic control. Ostrava. 2012. 118 p.

ТРИСТУПЕНЕВА ЕЛЕКТРИЧНА МАШИНА ТА РЕЖИМИ ЇЇ РОБОТИ

К.П. Акинін, докт. техн. наук, **В.Г. Кіреєв**, канд. техн. наук, **І.С. Петухов**, докт. техн. наук, **А.А. Філоменко**, канд. техн. наук

Інститут електродинаміки НАН України,
пр. Берестейський, 56, Київ, 03057, Україна

Статтю присвячено дослідженню режимів роботи електричної машини з триступеневим ротором (ЕМТР). Розглянуто структури ЕМТР із можливістю повороту осі обертання ротора за двома кутовими координатами в обмеженому діапазоні кутів повороту. Описано принцип роботи машини у складі малогабаритних швидкодіючих прецизійних систем виявлення та супроводу цілі. На підставі моделі електродинамічного стану ЕМТР розроблена структурна схема слідувальної системи для управління траєкторією руху ротора за двома координатами. Наведено приклади реалізації траєкторій руху ротора при лінійно наростаючому сигналі задання і при заданні, яке описується спіраллю Архімеда. Отримано залежності модулів відносної точності руху ротора за заданими траєкторіями від налаштувань системи. Бібл. 12, рис. 9, таблиця.

Ключові слова: система керування, траєкторії руху, електрична машина з триступеневим ротором.

Надійшла: 26.10.2023

Прийнята: 09.11.2023

Submitted: 26.10.2023

Accepted: 09.11.2023